

Voltammetric Determination of Trace Heavy Metals by Sequential-Injection Analysis at Plastic Fluidic Chips with Integrated Carbon Fibre-Based Electrodes

Vrysiida Partheni^a, Konstantinos Svarnias^a, Anastasios Economou^{a,*}, Christos Kokkinos^a, Peter R. Fielden^b, Sara J. Baldock^b, Nicholas J. Goddard^c

^a Department of Chemistry, National and Kapodistrian University of Athens, Athens 157 71, Greece

^b Department of Chemistry, Lancaster University, Lancaster, LA1 4YB, UK

^c Process Instruments (UK) Ltd, March Street, Burnley, BB12 0BT, UK

* e-mail: aeconomou@chem.uoa.gr

Received: ((will be filled in by the editorial staff))

Accepted: ((will be filled in by the editorial staff))

Abstract

This work describes a sequential injection analysis (SIA) method for on-line stripping voltammetric determination of Pb(II), Cd(II) and Zn(II) using an injection-moulded electrochemical fluidic chip consisting of 3 conductive carbon fibre-loaded polymer electrodes embedded in a plastic fluidic holder. The sample containing the target metals and a solution containing Bi(III) were aspirated in the holding coil of the SIA manifold. Then, the flow was reversed and the two solutions were directed to the fluidic cell through a mixing coil which induced mixing of the two zones. Upon reaching the cell, simultaneous reduction of the target metals and Bi(III) occurred resulting in the formation of a metal-Bi alloy on the working electrode. Finally, the accumulated metals were stripped off the bismuth-film electrode via a positive potential scan and the oxidation current was recorded. The experimental variables (concentration of the bismuth plating solution, deposition potential, sample volume, stripping mode) were investigated and the potential interferences were assessed. The limits of quantification were 2.8 $\mu\text{g L}^{-1}$ for Pb(II), 3.6 $\mu\text{g L}^{-1}$ for Cd(II) and 4.2 $\mu\text{g L}^{-1}$ for Zn(II) and the within-chip and between-chip % relative standard deviations were $\leq 6.3\%$ and $\leq 14\%$, respectively. Finally, the sensor was applied to the determination of trace metals in a fish food sample.

Keywords: injection moulding; bismuth-film electrode; stripping voltammetry; trace metals; sequential-injection analysis; carbon fibre electrode

DOI: 10.1002/elan.((will be filled in by the editorial staff))

1. Introduction

Heavy metals, such as Zn, Cd and Pb, are toxic species that can accumulate in living organisms via the consumption of food and water, breathing and absorption through the skin [1]. Since heavy metal species usually exist at trace levels in different samples, sensitive spectroscopic approaches are mainly used for their determination [1-3]. However, electroanalytical methods, and in particular stripping, analysis, exhibit some important advantages compared to optical techniques such as inexpensive and portable instrumentation, low power requirements and rapidity which increase their scope for field analysis [4-5].

Recent advances on novel types of electrochemical transducers, have enabled the replacement of toxic mercury electrodes with more environment-friendly "green" bismuth-, tin- or antimony-based electrodes in stripping analysis [6,7]. In particular, bismuth electrodes have attracted wide interest and have been shown to yield

electroanalytical performance comparable to that of mercury electrodes [8,9].

Several types of flow systems have been reported in order to perform on-line stripping analysis of trace heavy metals with the aim to improve the accuracy/precision, to reduce the consumption of samples and reagents and to automate the analytical protocol [10-13].

Injection-molding is an interesting universal approach for low-cost and high-throughput fabrication of plastic objects in different configurations. In particular, it enables the fabrication of electrochemical transducers using polymers reinforced with carbon nanomaterials. A plastic conductive electrode has been developed for the determination of Cu(II) [14] while an integrated 3-electrode fluidic device has been reported for on-line determination of Pb(II) [15]. However, these applications make use of bare carbon-based electrodes which do not provide multi-element capabilities. As a first step towards multi-element analysis, recently we have reported on the

use of a batch antimony-modified injection-molded electrochemical sensor for the determination of Pb(II) and Cd(II).

In the present work, we describe a semi-disposable electrochemical fluidic chip fabricated by an injection-moulding process. The chip consists of 3 conductive carbon fibre-loaded polymer electrodes embedded in a plastic fluidic holder. The devices were applied to the voltammetric determination of trace heavy metals using a sequential-injection analysis (SIA) manifold. During the analysis, the working electrode is electroplated *in situ* with a thin film of bismuth, enabling the simultaneous determination of Pb(II), Cd(II) and Zn(II) by anodic stripping voltammetry.

2. Experimental

2.1. Chemicals and reagents

All the chemicals were of analytical grade and purchased from Merck (Darmstadt, Germany) or Sigma-Aldrich (USA). Doubly-distilled water was used throughout. Stock solutions containing 10 and 100 mg L⁻¹ of different metals (Cd(II), Pb(II), Sn(II), Zn(II), In(III), Cu(II) and Tl(I)) were prepared from 1000 mg L⁻¹ standard solutions after appropriate dilution with water. The Bi(III) plating solution was 2.0 mg L⁻¹ in 0.10 mol L⁻¹ acetate buffer (pH 4.5). The carrier solution was 0.10 mol L⁻¹ acetate buffer (pH 4.5) prepared from sodium acetate and hydrochloric acid.

The fish food sample was purchased from a local pet store. 5.0 mL of concentrated HCl were added to 0.2500 g of sample and the sample was microwave-digested using in a CEM Mars 5 microwave (CEM Microwave Technology). The resulting solution was diluted to a final volume of 50.0 µL with 0.10 mol L⁻¹ acetate buffer (pH 4.5). The solution was analyzed before and after spiking with the target metals.

2.1. Instrumentation

The SIA manifold was assembled in house and is schematically illustrated in Figure 1. A 12-port valve (Vici-Valco, Switzerland) served as the selection valve. A Gilson MiniPuls3 peristaltic pump (Middleton, WI, USA) was used for solution handling. The electrodes of the electrochemical fluidic cell were connected to a home-made computer-controlled potentiostat. The valve, the pump and the potentiostat were interfaced to a PC through a NI 6025 E PCI multi-function interface card (National Instruments, Austin,

Texas). The connecting tubing was made of PTFE (0.7 mm i.d.). Control of the SIA apparatus and the potentiostat and data acquisition were accomplished by a program developed in-house using LabVIEW 8.6 (National Instruments) running in a PC under Windows 7. This program enabled complete automation of single or multiple stripping cycles.

A photograph of the fluidic cell is illustrated as an insert in Fig. 1 and its fabrication is described in the Supporting Information. All the electrodes are made of carbon fibre-loaded polystyrene and the reference electrode was further coated with AgCl.

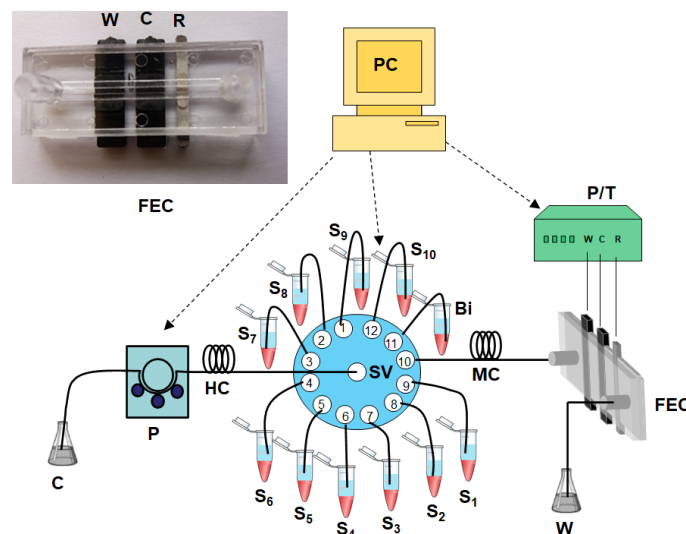


Fig. 1. Schematic illustration of the SIA manifold and the fluidic electrochemical cell (FEC) as an insert. C, carrier; P, pump; SV, selection valve; HC, holding coil; MC, mixing coil; P/T, potentiostat; PC, computer; S₁-S₁₀, samples or standards; Bi, Bi(III) plating solution; W, waste; W, working electrode; C, counter electrode; R, reference electrode.

2.2. Experimental procedure

The steps of the experimental sequence are summarized in Table 1. At the beginning of each working day, the manifold and the cell were rinsed with the 0.1 mol L⁻¹ acetate buffer (pH 4.5) carrier solution (step 1). A zone of the sample or standard was aspirated into the holding coil (step 2) followed by a zone of the Bi(III) (step 3). The flow was reversed and the sample zones were delivered to the electrochemical cell through the mixing coil for simultaneous determination of the target metals and bismuth (step 4). After a short equilibration period (step 5), a positive potential scan in the SW mode (frequency, 50 Hz; step increment, 4 mV; pulse height, 20 mV) was applied and the voltammogram was recorded from -1.4 to +0.2 V in

quiescent solution (step 6). Finally, the electrode was cleaned from traces of remaining metals at + 0.2 V in the flowing 0.1 mol L⁻¹ acetate buffer (pH 4.5) carrier solution (step 7). The electrode was then ready for a new stripping cycle. Each complete analysis cycle lasted 213 s and the sample throughput was 15 h⁻¹. All the measurements were carried out in the presence of dissolved oxygen.

Table 1. Step sequence with the final conditions for the analysis.

Step	Duration (s)	Flow rate (mL min ⁻¹)	Pump status	Valve position	Potential (V)
1[a]	120	1.8	Deliver	10	+0.2
2	40	1.8	Aspirate	1-9,12	+0.2
3	20	1.8	Aspirate	11	+0.2
4	120	1.2	Deliver	10	-1.4
5	5	0	Deliver	10	-1.4
6	8	0	Deliver	10	Scan -1.4 V to +0.2 V
7	20	1.8	Deliver	10	+0.2

[a] This step was only used at the beginning of each working day to rinse and fill the manifold with carrier.

3. Results and discussion

Examination of the bare injection-moulded electrode's surface with optical microscopy clearly shows the individual carbon fibres embedded in the plastic matrix (Figure 2(A)). For the purpose of microscopic examination, coating of the electrode's surface with a bismuth film was performed before assembling the fluidic cell using a 100 mg L⁻¹ Bi(III) solution in 0.1 mol L⁻¹ acetate buffer (pH 4.5) at -1.4 V for 120 s. After coating with bismuth, the electrode surface is completely covered by the metal coating (Figure 2(B)). This indicates that a bismuth film can be successfully deposited on the surface of the conductive electrodes.

The study of the working conditions involved: the concentration of the Bi(III) solution; the deposition potential; the sample volume, and; the voltammetric stripping mode.

The effect of the Bi(III) solution concentration used for the *in-situ* formation of the Sb-film on the stripping peak currents of Pb, Cd and Zn is illustrated in Fig. 3(A); a Bi (III) concentration of 2 mg L⁻¹ was selected as it provided the highest stripping signal for the three target metals.

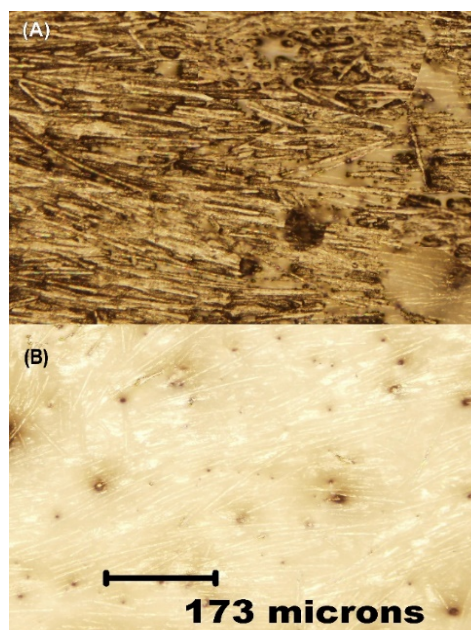


Fig. 2. Optical microscopy showing the surface morphology of: an injection-moulded electrode before (A) and after (B) coating with a bismuth film.

The effect of the volume of the sample zone on the stripping peak currents of Pb, Zn and Cd is illustrated in Fig. 3(B) indicating an almost linear increase in the signals with the sample volume in the range examined (200-1200 μ L). A sample volume of 1200 μ L was normally used but still larger volumes could be employed to improve the sensitivity.

The effect of the deposition potential on the stripping peak currents of Pb, Cd and Zn is illustrated in Fig. 3(C). The signals increased as the deposition potential became more negative suggesting higher deposition efficiency at more cathodic deposition potentials. However, at potentials more negative than -1.4 V, the signals started to decrease and this was attributed to the formation of H₂ bubbles on the surface which inhibited the deposition process; therefore, a deposition potential of -1.4 V was selected.

Different scanning waveforms were investigated for the stripping step (Fig. 3(D)). The linear sweep (LS) mode produced a sloping baseline and the sensitivity of the differential pulse (DP) mode was low. The square wave (SW) mode combined adequate sensitivity and a flat baseline and was selected for further experiments.

volume; (C) the deposition potential; (D) the scanning waveform. Conditions: concentration of target metals, 40 $\mu\text{g L}^{-1}$.

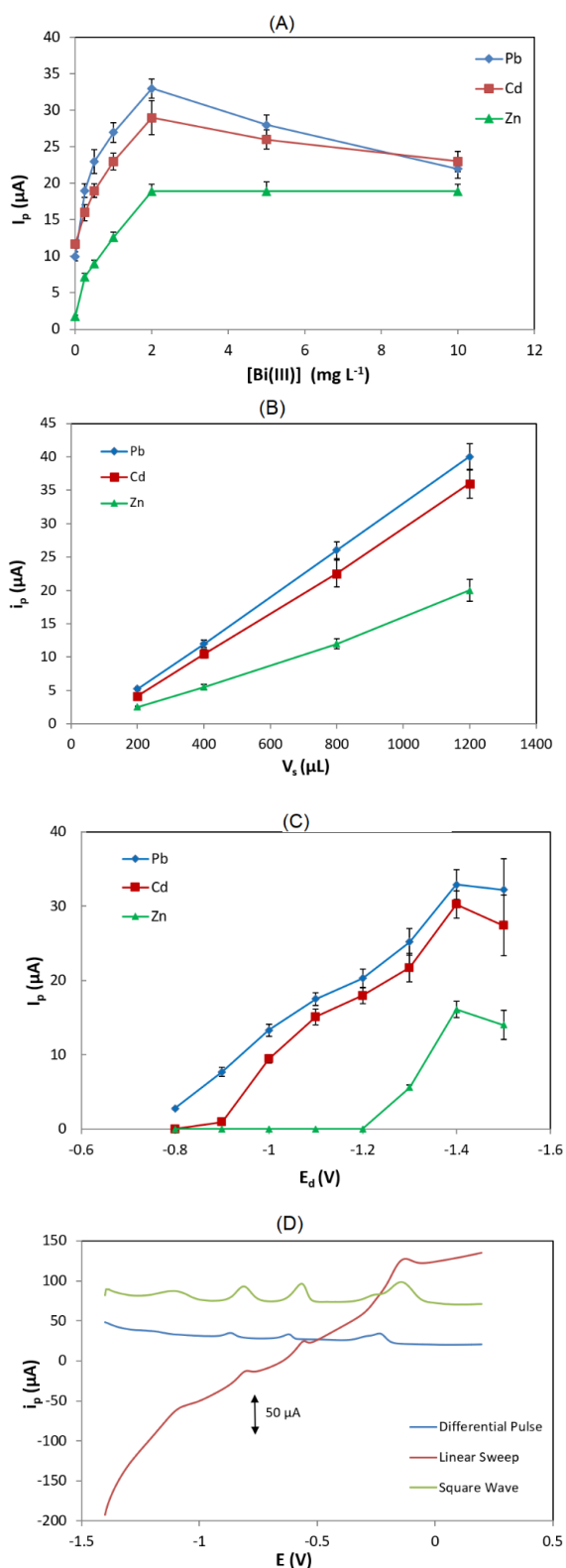


Fig. 3. Effect of different experimental parameters: (A) the concentration of the Bi(III) plating solution; (B) the sample

Calibration for Cd(II), Pb(II) and Zn(II) was performed in the concentration range 0-140 $\mu\text{g L}^{-1}$. The calibration features (calibration equation, coefficient of determination and limits of quantification) for the target metals are summarized in Table 2. The limit of quantification (LOD) for each metal was calculated from the equation: $\text{LOQ} = 10 \times s_b / S$ (where s_b is the standard deviation of the intercept of the calibration plot and S is the slope of the calibration plot); the LOQs were verified experimentally as illustrated in Fig. S1 (Supporting Information). A representative series of voltammograms and the respective calibration plots are illustrated in Figure 4.

Table 2. Calibration features of the three target metals.

	Calibration equation	R[a]	LOQ [b] ($\mu\text{g L}^{-1}$)
Cd(II)	$I_p (\mu\text{A}) = (0.935 \pm 0.11) C_{\text{Cd}} (\mu\text{g L}^{-1}) + (1.22 \pm 0.27) (\mu\text{A})$	0.998	2.8
Pb(II)	$I_p (\mu\text{A}) = (0.975 \pm 0.014) C_{\text{Pb}} (\mu\text{g L}^{-1}) + (1.62 \pm 0.35) (\mu\text{A})$	0.997	3.6
Zn(II)	$I_p (\mu\text{A}) = (0.425 \pm 0.007) C_{\text{Zn}} (\mu\text{g L}^{-1}) + (0.09 \pm 0.19) (\mu\text{A})$	0.997	4.4

[a] coefficient of determination. [b] limit of quantification

The within-chip precision was calculated by performing 8 repetitive measurements with a solution containing 20 $\mu\text{g L}^{-1}$ of the target metals using the same chip and the the % relative standard deviations were 5.2 % for Pb(II), 5.9 % for Cd(II) and 6.3 % for Zn(II).

The between-chip reproducibility was calculated by performing measurements with a solution containing 20 $\mu\text{g L}^{-1}$ of the target metals at 5 different; the % relative standard deviations were 12.5 % for Pb(II), 13.1 % for Cd(II) and 14.0 % for Zn(II).

The long-term stability of the chips was assessed by measuring the peak heights of the target metals for 20 repetitive measurements on a single chip. The peak heights were statistically stable, indicating that the chips could be used in a semi-disposable manner.

The stability of the reference electrode was also assessed. It was found that using a 0.10 mol L^{-1} acetate buffer (pH 4.5) carrier solution prepared from ammonium acetate and acetic acid resulted in instability of the reference electrode. Using a 0.10 mol L^{-1} acetate buffer (pH 4.5) carrier solution prepared from sodium acetate and hydrochloric acid (in order to achieve a constant Cl^- concentration) stabilized the potential of

the AgCl electrode and peak potentials shifted by less than 3%.

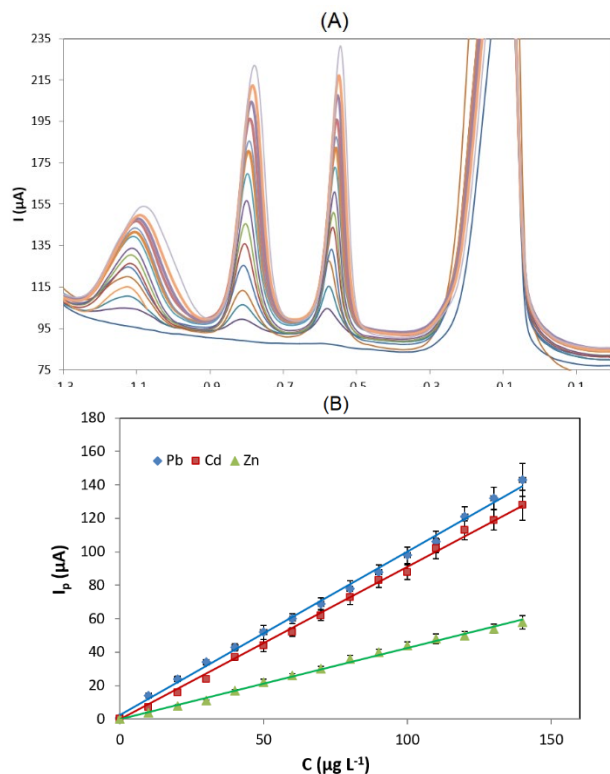


Fig. 4. (A) Stripping voltammograms for the determination of Pb(II), Cd(II) and Zn(II) in standard solution in the concentration range 0–140 $\mu\text{g L}^{-1}$; (B) Respective calibration plots.

The effect of common cations that could potentially interfere with the determination of the target metals (i.e. Sn(II), Sb(III), In(III), Tl(I) and Cu(II)) was studied. Sn(II) and Sb(III) did not statistically interfere. Tl(I) and In(III) interfered severely by producing stripping peaks that overlapped with the Cd peak (Fig. S2, Supporting Information); however, the concentration of these cations in the vast majority of typical samples is very low. The most serious interference was Cu(II), which can be present at high concentrations in many samples and caused a significant suppression of all the peaks (Fig. S2, Supporting Information). It has been shown previously that ferrocyanide anions can alleviate the Cu(II) interference for Pb(II) and Cd(II) by suppressing the Cu peak and this was true in the case of the present work (Figure S3, Supporting Information). However, ferrocyanide also suppresses the Zn peak as illustrated in Figure S3 and therefore, cannot be used as a masking agent for Zn [17,18].

To assess the analytical utility of the method, Cd and Pb were determined in a digested fish food sample. Addition of ferrocyanide to the sample was necessary to alleviate interference by Cu and therefore simultaneous of Zn(II) was not possible, as mentioned in the previous paragraph. Preliminary analysis indicated that the Pb(II) and Cd(II) concentrations in the digested sample were lower than the LOQ of the method and the accuracy was estimated by spiking the sample with 20 $\mu\text{g L}^{-1}$ of Pb(II) and Cd(II) and calculating the recoveries. Quantification of Pb(II) and Cd(II) was performed by the method of multiple standard additions. Voltammograms of the digested sample and standard additions plots are illustrated in Fig. 5; the recoveries were $103 \pm 7\%$ for Cd and $105 \pm 8\%$ for Pb ($n=3$). It is interesting that, in this sample, the sensitivity for Pb(II) was lower than the sensitivity for Cd(II) which was attributed to matrix effects; however, these were accounted for by the method of standard additions.

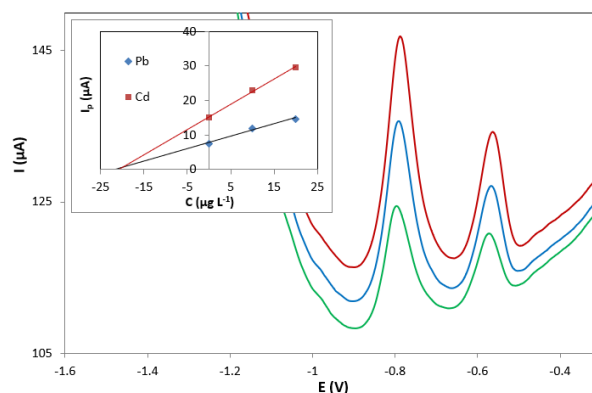


Fig. 5. Stripping voltammograms for the determination of Pb and Cd in a fish food sample spiked with 20 $\mu\text{g L}^{-1}$ each of Pb(II) and Cd(II) (the standard additions plot is shown as an insert). $2.0 \times 10^{-5} \text{ mol L}^{-1}$ of $\text{K}_4[\text{Fe}(\text{CN})_6]$ was added in the sample.

4. Conclusions

An automated sequential-injection analysis/anodic stripping voltammetry method has been developed for the simultaneous determination of Zn(II), Cd(II) and Pb(II). Injection-moulded fluidic chips were used which incorporate three conductive plastic electrodes; the working electrode was coated *in situ* with a thin bismuth film to improve the detection sensitivity. The limits of quantification for the three target metals were at the low $\mu\text{g L}^{-1}$ levels, the within-chip standard deviation was $<6.5\%$ and the between-chip standard deviation was $<15\%$. The chips are reusable for at least 20 analytical cycles. It is envisaged that the fluidic chips will be used for additional flow-through applications in combination

with other electrogenerated metal-film electrodes (such as gold films and antimony films).

5. References

- [1] T. Bhattacharjee, M. Goswami, *Int. J. Eng. Sci. Invention* **2018**, *7*, 12-21.
- [2] E. Bulska, A. Rusczyńska, *Phys. Sci. Rev.* **2017**, 20178002
- [3] A.B.M. Helaluddin, R. Saadi Khalid, M. Alaama, S. Atif Abbas, *J. Pharm. Res.* **2016**, *15*, 427-434
- [4] A. Economou, C. Kokkinos, in *Electrochemical Strategies in Detection Science, Vol. 6* (Ed: D.W.M Arrigan), The Royal Society of Chemistry: UK, **2016**, pp. 1-18.
- [5] A.J. Borrill, N.E. Reily, J.V. Macpherson, *Analyst* **2019**, *144*, 6834-6849.
- [6] C. Arino, N. Serrano, J.M. Díaz-Cruz, M. Esteban, *Anal. Chim. Acta* **2017**, *990*, 11-53.
- [7] G.M.S. Alves, L.S. Rocha, H.M.V.M. Soares, *Talanta* **2017**, *175*, 53-68
- [8] V. Jovanovski, S.B. Hočevan, B. Ogorevc, *Curr. Opin. Electroche.* **2017**, *1*, 114-122.
- [9] I. Švancara, C. Prior, S.B. Hočevan, J. Wang, *Electroanalysis*, **2010**, *22*, 1405-1420.
- [10] K. Keawkim, S. Chuanuwatanakul, O. Chailapakul, S. Motomizu, *Food Contr.* **2013**, *31*, 14-21.
- [11] W. Wonsawat, S. Chuanuwatanakul, W. Dungchai, E. Punrat, S. Motomizu, O. Chailapakul, *Talanta* **2012**, *100*, 282-289.
- [12] W. Siringkhawut, K. Grudpan, J. Jakmunee, *Talanta* **2011**, *84*, 1366-1373.
- [13] A. Economou, *Anal. Chim. Acta* **2010**, *683*, 38-51.
- [14] N. Gharib Naseri, S.J. Baldock, A. Economou, N.J. Goddard, P.R. Fielden, *Electroanalysis* **2008**, *20*, 448-454.
- [15] C. Kokkinos, A. Economou, N.J. Goddard, P.R. Fielden, S.J. Baldock, *Talanta* **2016**, *153*, 170-176.
- [16] S. Christidi, A. Chrysostomou, A. Economou, C. Kokkinos, P.R. Fielden, S.J. Baldock, N.J. Goddard, *Sensors* **2019**, *19*, 4809.
- [17] D. Yang, L. Wang, Z. Chen, M. Megharaj, R. Naidu, *Electroanalysis* **2013**, *25*, 2637-2644.
- [18] C. Kokkinos, A. Economou, I. Raptis, C.E. Efstathiou, *Electrochim. Acta* **2008**, *53*, 5294-5299.